

Design of experiments for thermo-mechanical behavior of polypropylene/high-density polyethylene/nanokaolinite clay composites

R. Anjana · Asha K. Krishnan ·
Tresa Sunitha Goerge · K. E. George

Received: 7 May 2013 / Revised: 25 August 2013 / Accepted: 3 September 2013 /
Published online: 1 November 2013
© Springer-Verlag Berlin Heidelberg 2013

Abstract This paper deals with the preparation of nanocomposites using polypropylene (PP)/high-density polyethylene (PE) blend and low-cost nanokaolinite clay by melt compounding in a Thermo Haake Rheocord mixer. The optimization of processing parameters and nanoclay content is done using Box–Behnken design of response surface methodology. Mechanical properties are modeled in terms of processing parameters and nanoclay content and results are verified using statistical analysis. Most reports suggest that kaolinite clay is difficult to disperse in polymer matrix compared to costly montmorillonite clay. This difficulty is overcome by surface modification of nanokaolinite clay by an organic group and the effect of modification is studied using melt flow index, thermal stability and dynamic mechanical behavior. Morphological characterization is done by scanning electron microscopy and X-ray diffraction. Study shows that cheap and abundantly occurring nanokaolinite clay is an efficient reinforcing agent for PP/PE blend. Design of experiments can be effectively used to model such a system, which is influenced by a number of variables. It is also observed that surface modification of the nanoclay with an organic group leads to remarkable improvement in the thermal and mechanical properties of the blend.

Keywords Nanokaolinite clay · Box–Behnken design · Surface modification · Thermogravimetric analysis · Dynamic mechanical behavior

R. Anjana · A. K. Krishnan · T. S. Goerge · K. E. George (✉)
Department of Polymer Science and Rubber Technology, Cochin University of Science and
Technology, Kochi, Kerala 682022, India
e-mail: kegeorge@cusat.ac.in

R. Anjana
e-mail: anjan.rnair@gmail.com

R. Anjana
Department of Chemical Engineering, Government Engineering College, Thrissur,
Kerala 680009, India

Introduction

Polymers are widely used owing to their ease of production, lightweight and ductile nature. However, compared to metals and ceramics, they are inferior in mechanical properties. One way to improve their mechanical properties is to reinforce them with particulate fillers such as talc, mica, calcium carbonate, kaolin, fumed silica or fibers of glass, nylon, etc. Nanofillers have now emerged as the ultimate reinforcing agents for polymers for improving their mechanical properties without affecting density, transparency and processibility [1–4]. Polymer nanocomposites (PNC) are a new family of materials that have attracted great interest in industry and academy. They are ideal candidates for a vast majority of structural and functional material applications [5]. Polypropylene (PP) and high-density polyethylene (PE) are most widely used commodity plastics owing to their lightweight, ease of production and processibility. Blending and incorporation of a nanofiller can uplift the applicability of PP and PE as a strategic material. These nanoparticles are dispersed in the polymer matrix at a relatively low concentration (often under 6 % by weight), thereby producing materials of lower density and better processibility [6]. As the nanoparticles are so small and their aspect ratios are very high, they are capable of improving polymer properties such as stiffness, heat deflection temperature, dimensional stability, gas barrier properties, electrical conductivity and resistance to flammability of the polymer matrix even at low loadings [7].

Polymer layered silicate nanocomposites are currently prepared in four ways: in situ polymerization [8], intercalation from a polymer solution [9, 10], direct intercalation by molten polymer [11, 12] and sol–gel technology [13]. According to Ray and Okamoto [14], direct intercalation by molten polymer method of preparation of nanocomposites has greater advantages over other methods as this method is environmentally benign owing to the absence of organic solvents and is compatible with current industrial process, such as extrusion and injection molding. PNC made of silica, montmorillonite clay and other nanoparticles are extensively studied and reported in earlier studies [15–23]. However, scarce amount of literature is available on effect of nanokaolinite clay as reinforcing agent on thermoplastics. Kaolinite clay has a wide variety of applications in industry, particularly as filler in paper, plastics, paints and rubber. It was observed in a recent report that the china clay-based PNCs give better oxygen barrier and water transport property than that from montmorillonite-based nanoclay. Kaolinite has the potential to an ideal precursor for the preparation of PNC since it is cheaper when compared to montmorillonite clays. [24]. The main challenge facing the preparation of PNCs using nanoclay is that clay is naturally hydrophilic, whereas PP and PE have no polar groups in their backbone and are the most hydrophobic polymers. In order to overcome this difficulty and to ensure proper dispersion, either compatibilizers are used to provide a bridge between clay and polymer [11, 16, 17, 20, 22, 23, 25–27] or clay surface modifiers are used to replace the inorganic cations (Na^+) with organic cations like dialkyl ammonium, alkyl amine, etc. [4, 21, 28, 29].

Response surface methodology (RSM) is a statistical technique that is used for modeling and optimization of processes in which the response of interest is influenced by several variables. The RSM has important applications not only in the

design, development, and formulation of new processes, but also in the improvement of existing designs. It defines the effect of independent variables on the process either individually or collectively. The technique is employed extensively for optimization studies in recent years. RSM involves three steps: performing the statistically designed experiments, estimating coefficients in the proposed model and predicting the response of the process, and checking the validity of the model. The Box–Behnken design (BBD) is the most popular class of second-order designs of RSM. This design is well suited for fitting quadratic surfaces and usually works well for process optimization. The design of experiments using RSM was successfully employed for the optimization of process parameters by some researchers in their studies like polystyrene/montmorillonite composites [30], styrene/butadiene/rubber/organoclay composites [31], NBR-layered silicate nanocomposites [32] and PP/nanoclay/CaCO₃ nanocomposites [20]. In the present study, BBD with three factors at three levels was applied and simulations carried out using Minitab 14 software. The three parameters mixing temperature, mixing torque and nanoclay content are denoted as X_1 , X_2 , and X_3 , respectively. The experimental ranges of factors giving the maximum range of mechanical properties were found by conducting preliminary experiments.

The objective of this study was to investigate the effect of low-cost nanokaolinite clay as a reinforcing agent for the improvement of thermal and mechanical properties of a typical PP/PE blend. It is also proposed to explore the effect of melt compounding parameters and nanoclay loading for nanocomposite system with optimized mechanical properties and the influence of the above-mentioned parameters on the mechanical properties of PP/PE/organoclay; nanocomposites were statistically investigated using Box–Behnken experimental design approach to obtain this end. The effect of surface modification of nanoclay on the nanocomposites morphology and thermal behavior was also studied by melt flow indexer, thermogravimetric analysis (TGA), dynamic mechanical analyzer (DMA), scanning electron microscopy (SEM) and X-ray diffraction (XRD).

Experimental setup

Materials

The materials used for this study are Polypropylene-MFI-25 (230 °C/2.16 kg) and high-density polyethylene-MFI-20 (190 °C/2.16 kg), supplied by Reliance polymers Ltd., Mumbai. Nanokaolinite clays both unmodified clay (Nanocaliber 100) and surface modified clay with amino silane group (Nanocaliber 100 A), and BET-specific surface area 28–30 m²/g were supplied by English India Clays Ltd. India, with specifications given in Table 1.

Method of preparation

80 PP/20 PE by weight blends containing 1, 2 and 3 wt% organo-modified nanoclay were melt compounded in a Thermo Haake Rheocord at three different temperatures

Table 1 Characteristics of nanoclay

Average particle size	Bulk density	Plate thickness (SEM)
100 ± 5 nm	0.2–0.3 g/cc	<80 nm

Table 2 Variables in Box–Behnken design

Variables	Levels used, actual (coded)		
	Low (−1)	Medium (0)	High (1)
Mix temperature (°C) (X_1)	150	160	170
Mix torque (rpm) (X_2)	30	60	70
Nanoclay content (wt%) (X_3)	1	2	3

(150, 160, 170 °C) and using three different rotor speeds (30,50,70). The mixing was done for a uniform time of 8 min. The total weight of material per batch was 40 g, which gives a suitable volume for the Rheocord. All the process variables (temperature, rpm and nanoclay loading) were varied in three levels suggested by three level-three factor BBD as shown in Table 2. The mixing parameters and nanoclay content were varied according to a predetermined set of 15 experiments as specified by Box–Behnken experimental design as shown in Table 3. For investigating the effect of surface modification, nanocomposites are prepared with unmodified nanoclay at 2 wt%. Nanoclays were preheated for 45 min before mixing to get rid of trapped moisture content. The resulting composites were hot pressed into sheets and cut into pieces. The material was then injection molded using a plunger-type laboratory injection-molding machine with a barrel temperature of 180 °C.

Method of characterization

Tensile and flexural properties were evaluated using Shimadzu Autograph AG-I series Universal testing machine with a load cell capacity of 10 kN according to ASTM D 638 [33] and ASTM D 790 [34], respectively. Tensile samples are injection-molded, dumbbell-shaped specimens with an overall length of 115 mm, a width in the gauge section of 8 mm and thickness of 3.2 ± 0.4 mm. Izod impact test on un-notched rectangular bar samples was carried out following ASTM D 256 [35] test method on a pendulum-type RESIL IMPACT JUNIOR (CEAST). Melt flow index (MFI) determined using CEAST Modular Line Melt Flow Indexer according to ASTM D 1238 [36]. Flexural and impact specimens are rectangular bars of dimensions $40 \times 12 \times 3.2$ mm³ (width \times length \times thickness). A minimum of five samples were tested in each nanocomposites and the average results were recorded.

Thermal stability of PP/PE (80/20) blend, unmodified and modified clay nanocomposites was analyzed. Thermal analysis was done in a TA-Q 600 series instrument in nitrogen atmosphere for samples of 5–7 mg size and temperature range of 400–1,020 °C at 20 °C/min. The dynamic mechanical properties were determined using dynamic mechanical thermal analyzer [DMTA; Model 2980 supplied by TA Instrument (USA)]. The test sample is a rectangular strip of

Table 3 Box–Behnken experimental design table with experimental response values of mechanical properties

Sl. no.	Temperature (°C) (X_1)	Mixing torque (rpm) (X_2)	Nanoclay content (wt%) (X_3)	Tensile strength (N/mm ²)	Tensile modulus (N/mm ²)	Flexural strength (N/mm ²)	Impact strength (kJ/mm ²)
1.	150	50	1	37.0	1,283.52	42.05	23.45
2.	160	70	3	36.5	1,322.71	43.35	22.64
3.	170	50	1	33.2	1,252.05	42.03	24.25
4.	170	30	2	32.6	1,298.32	43.78	22.33
5.	160	50	2	37.9	1,390.65	45.20	22.01
6.	160	30	3	36.6	1,331.45	43.35	22.56
7.	160	50	2	38.1	1,390.45	45.65	22.13
8.	160	70	1	36.1	1,311.54	43.45	22.24
9.	150	70	2	34.2	1,289.20	42.43	23.75
10.	160	50	2	38.0	1,390.84	45.78	22.00
11.	170	50	3	32.6	1,261.14	42.56	24.64
12.	170	70	2	33.1	1,248.72	42.00	24.91
13.	150	50	3	35.3	1,296.58	42.34	23.54
14.	150	30	2	34.5	1,313.15	42.76	23.65
15.	160	30	1	36.6	1,321.52	43.04	23.01

dimension $40 \times 12 \times 3.2 \text{ mm}^3$. The dual-cantilever mode of deformation was used under the test temperature range from 40 to 110 °C with a heating rate of 30 °C/min at a constant frequency of 10 Hz. The morphology of the tensile fractured cross section was examined using a scanning electron microscope JEOL-JSM-6390 with an accelerator voltage of 20 kV in a vacuum atmosphere. The samples were subjected to gold sputtering prior to electron microscopy to give necessary conductivity. The samples were also analyzed in a Bruker AXS D8 Advance X-Ray Powder Diffractometer (Cu K α radiation) to find the basal spacing of nanocomposites. The samples were scanned in the range of 3°–80° at incremental step of scanning 0.02° at a wavelength of 1.5406 Å.

Results and discussion

Optimization of mechanical properties

The Box–Behnken method of RSM is an efficient statistical experimental design tool for the optimization of three or more process variables with limited number of experiments. In this study, three level-three factor Box–Behnken experimental design was used which suggests a set of 15 experiments. The process variables studied are temperature and rotor speed of mixing and nanoclay content. The experimental domain as presented in Table 2 was determined from the results of the preliminary runs. The mechanical properties optimized are tensile strength, tensile

modulus, flexural strength and impact strength. The Box–Behnken experimental design table with the mechanical properties analyzed is given in Table 3.

The experimental responses of the BBD are fitted with a second-order polynomial model as shown in the following equation:

$$Y = \beta_0 + \beta_1 X_1 + \beta_2 X_2 + \beta_3 X_3 + \beta_{11} X_1^2 + \beta_{22} X_2^2 + \beta_{33} X_3^2 + \beta_{12} X_1 X_2 + \beta_{13} X_1 X_3 + \beta_{23} X_2 X_3 \quad (1)$$

where Y is the response variables of mechanical properties; β_0 a constant; β_1 , β_2 and β_3 the regression coefficients for linear effects; β_{11} , β_{22} and β_{33} the quadratic coefficients; and β_{12} , β_{13} and β_{23} are the interaction coefficients. The coefficients of the model in coded terms for tensile strength, tensile modulus, flexural strength and impact strength are given in Table 4. The significance of the regression coefficients was analyzed using the p and t test. The values of p , t , and the significance level $(1 - p)$ are given in Table 4. It can be observed from Table 4 that all of the terms, except for the interaction terms, are highly influential in the model for the prediction of tensile, flexural and impact properties of the composite as the significance level is greater than 95 %.

The results of analysis of variance (ANOVA) test for tensile strength presented in Table 5 show a higher degrees of freedom (F) value for regression (11.51) than the tabulated value of 8.81, but the F value obtained for lack of fit, 84.27, is higher than the tabulated value of 8.81. This shows that the quadratic model can navigate the design space well. It is evident from the ANOVA table that all terms except interaction have a p value < 0.05 and have significant effect on the mechanical properties.

Statistical verification of model

The predictability of the model quantified in terms of standard statistical performance evaluation measures such as correlation coefficient (R), average absolute relative error (AARE), average root-mean-square error (RMSE), normalized mean-biased error (NMBE) and scatter index (SI) are expressed in the following equations:

$$R = \frac{\sum_{i=1}^N (E - \bar{E})(P_i - \bar{P})}{\sqrt{\sum_{i=1}^N (E_i - \bar{E})^2 \sum_{i=1}^N (P_i - \bar{P})^2}} \quad (2)$$

$$\text{AARE}(\%) = \frac{1}{N} \sum_{i=1}^N \left| \frac{(E_i - P_i)}{E_i} \right| \times 100 \quad (3)$$

$$\text{RMSE} = \left[\frac{1}{N} \sum_{i=1}^N (P_{ij} - E_{ij})^2 \right]^{1/2} \quad (4)$$

Table 4 Estimated regression coefficients and corresponding t and p values for mechanical properties

Factor	Coefficient of the model in uncoded factors	t value	p value	Significance level (%)
(a) Tensile strength				
β_0	-865.800	-38.943	0.000	>99
β_1	11.244	41.086	0.000	>99
β_2	0.047	1.672	0.032	>96
β_3	9.631	7.038	0.001	>99
β_{11}	-0.035	-41.447	0.000	>99
β_{22}	-0.002	-10.252	0.000	>99
β_{33}	-0.685	-8.049	0.000	>99
β_{12}	0.001	2.446	0.098	>90
β_{13}	-0.044	-5.350	0.103	>89
β_{23}	0.005	1.131	0.309	>68
(b) Tensile modulus				
β_0	-18,398.7	-15.269	0.000	>99
β_1	243.1	16.392	0.000	>99
β_2	11.4	3.027	0.029	>97
β_3	186.2	2.511	0.054	>95
β_{11}	-0.8	16.452	0.000	>99
β_{22}	-0.1	-5.942	0.002	>99
β_{33}	-41.4	-8.982	0.000	>99
β_{12}	0.0	-1.447	0.208	>79
β_{13}	-0.1	-0.224	0.832	>17
β_{23}	0.0	0.070	0.747	>25
(c) Flexural strength				
β_0	-473.032	-7.613	0.001	>99
β_1	6.254	8.176	0.000	>99
β_2	0.508	2.622	0.047	>95
β_3	4.912	1.284	0.055	>94
β_{11}	-0.019	-8.100	0.000	>99
β_{22}	-0.002	-3.675	0.014	>98
β_{33}	-1.372	-5.766	0.002	>99
β_{12}	-0.002	-1.586	0.174	>82
β_{13}	0.006	0.263	0.803	>19
β_{23}	-0.005	-0.449	0.673	>32
(d) Impact strength				
β_0	428.918	4.994	0.004	>99
β_1	-4.902	-4.636	0.006	>99
β_2	-0.537	-2.004	0.101	>89
β_3	-3.429	-0.649	0.045	>95
β_{11}	0.015	4.518	0.006	>99
β_{22}	0.000	0.389	0.713	>28
β_{33}	0.438	1.332	0.240	>76
β_{12}	0.003	1.963	0.107	>89
β_{13}	0.007	0.237	0.822	>17
β_{23}	0.011	0.673	0.531	>46

Table 5 Analysis of variance (ANOVA) for tensile strength

Source	Degrees of freedom	Sum of squares	Mean squares	<i>F</i>	<i>P</i>
Regression	9	52.8042	5.8671	11.51	0.008
Linear	3	35.8851	11.9617	23.47	0.002
Square	3	40.6389	13.5462	26.58	0.002
Interaction	3	0.5249	0.1750	0.34	0.796
Residual error	5	2.5480	0.5096		
Lack of fit	3	2.5280	0.8427	84.27	0.012
Pure error	2	0.0200	0.0100		
Total	14	55.3522			

$$\text{NMBE}(\%) = \frac{\frac{1}{N} \sum_{i=1}^N (E_i - P_i)}{\frac{1}{N} \sum_{i=1}^N E_i} \times 100 \quad (5)$$

$$\text{SI} = \frac{\text{RMSE}}{\bar{E}} \quad (6)$$

where E is the experimental finding and P is the predicted value obtained from the model. \bar{E} and \bar{P} are the mean values of E and P , respectively. N is the total number of data points employed in the investigation. The values of the statistical terms are presented in Table 6. The correlation coefficient is a commonly used statistic and provides information on the strength of the linear relationship between experimental and predicted values. The closeness of R toward unity indicates better fitting of the model toward experimental data. The AARE and RMSE are computed through a term-by-term comparison of the relative error and therefore are unbiased statistics for measuring the predictability of a model. The NMBE provides information on the mean bias in predictions from a model. A positive NMBE indicates over prediction, whereas a negative NMBE indicates under prediction from a model. It can be seen from the table that NMBEs for all mechanical properties except tensile modulus are low values and sufficiently able to predict the corresponding responses with better levels of accuracy [37]. The scatter index provides deviation from a linear behavior and small value indicates better performance of the model. Low values of SI indicate that the model fits with the experimental data without much scattering. From the statistical evaluation, it is clear that the model fits with the experimental data very well for all mechanical properties except tensile modulus.

Combined effect of variables on mechanical properties

The results of main experimental runs on the mechanical properties of nanocomposites are presented in Fig. 1a–d which are contour plots with lines or contours passing through points of equal magnitude. Each contour plot exhibits the variation of a property with respect to two variables with the others held at a constant value called as hold value to impart two-dimensional nature. The circular nature of contours with increasing magnitude shows that there exists a maximum value in the

Table 6 Standard statistical evaluation during validation of the model performance

Statistical parameter	Tensile strength	Tensile modulus	Flexural strength	Impact strength
<i>R</i>	0.97671282	0.60009523	0.977014108	0.913588747
ARRE (%)	0.963947035	67.71269713	0.539221041	1.361554074
RMSE	0.412148425	892.4622898	0.263895168	0.380939377
NMBE (%)	0.003241141	67.57976829	0.00253382	0.038456993
SI	0.011615923	0.679166101	0.006092044	0.016454317

experimental domain [20, 30–32]. It is evident from the figure that the tensile strength increases as temperature, clay content and mixing shear increase, reaches a maximum and then decreases. There is 16 % increase in tensile strength, 11 % increase in tensile modulus and 9 % increase in flexural strength. The enhancement of properties can be ascribed to the resistance exerted by clay sheets against plastic deformation of the polymer [33, 38]. The insertion of polymer chains inside the kaolinite sheets leads to an increase in the surface area of interaction between the clay and polymer matrix, thereby resulting in an increase in strength and modulus. The decrease in the mechanical properties after the critical loading may be due to the agglomeration of clay particles [34–36, 39]. When the clay agglomerates are present, the stress acting on a small part of the material surface would be much greater than the average stress applied to the test specimen. Even though there is a slight decrease in impact strength, this can be attributed to the increase in crystallinity on the addition of nanoparticles. Liu et al. [40] has reported similar effects. The increase in mechanical properties on increasing temperature and mixing shear can be attributed to proper mixing and dispersion of nanoclay sheets in the polymer matrix and better compatibilization of PP and PE blend [41–43]. Above critical temperature and mixing shear, the material degrades resulting in the decrease of mechanical properties.

As a result of optimization process, maximum enhancement in mechanical properties is obtained at a temperature of 160 °C, mixing shear of 50 rpm and 2 wt% nanoclay loading.

Effect of modification of nanokaolinite clay

Hydrophilic nature of nanokaolinite clay and organophilic nature of polymer matrix introduces difficulty in proper dispersion and compatibility of the polymer matrix and nanoclay, which results in poor mechanical and thermal properties of the resultant nanocomposites. This difficulty can be overcome either by adding different compatibilizers [11, 16–19, 22, 24, 41, 47] (which act as a bridge between the polymer chains and clay layer) or by modifying nanoclay (by replacing the inorganic cation of nanoclay with organic groups using ion exchange method) [21, 38, 39, 48, 49]. Here the properties of unmodified nanokaolinite clay composites are compared with the commercially available modified nanoclay, which replaces the inorganic cation with amino silane using guest displacement method. Dimethyl sulfoxide or urea is initially used as a guest intercalant to force in between clay

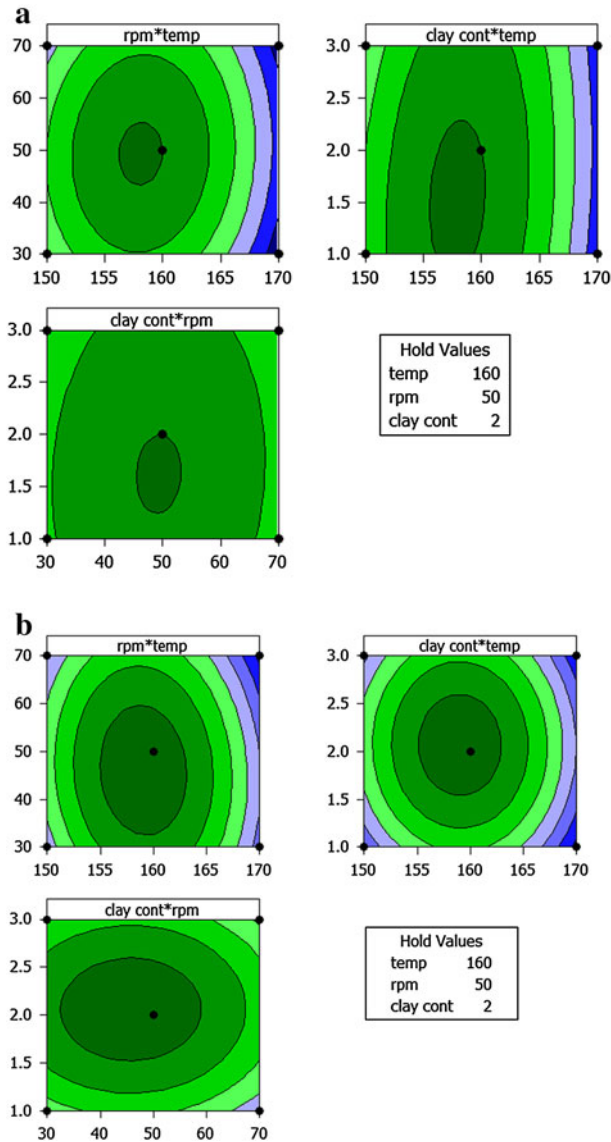


Fig. 1 **a** Contour plots of tensile strength. **b** Contour plots of tensile modulus. **c** Contour plots of flexural strength. **d** Contour plots of impact strength

platelets. Then, it is again treated with required organic molecule and the guest is displaced.

Mechanical properties

The mechanical properties of nanocomposites with both types of nanoclay at optimum processing conditions are compared with PP/PE pure blend and are

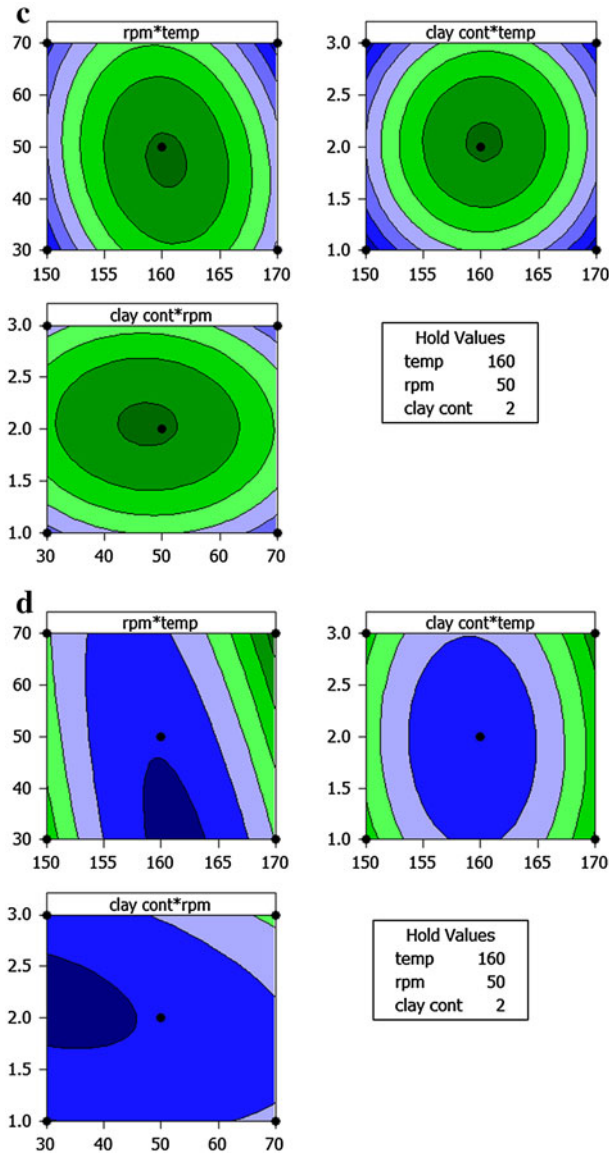


Fig. 1 continued

illustrated in Table 7. It is evident from the table that the nanocomposites have better mechanical properties such as tensile strength, tensile modulus and flexural strength than PP/PE pure blend. Surface modification of nanoclay further increases the mechanical properties. This can be attributed to better dispersion of nanofiller on the polymer matrix. This is evident in the morphological characterization using SEM.

Table 7 Mechanical properties of PP/HDPE nanocomposites

Property	PP/HDPE	PP/HDPE/N100	PP/HDPE/N100A
Tensile strength (N/mm ²)	34.91	36.59	38.1
Tensile modulus (N/mm ²)	1,091.45	1,252.33	1,390.45
Flexural strength (N/mm ²)	39.61	43.79	45.65
Impact strength (kJ/mm ²)	23.42	20.45	22.13

Melt flow index (MFI)

The MFI is a widely used rheological property and, occasionally, the stand-alone rheological information used in the industry. The presence of interactions between the polymer chains and silicate surface may affect the mobility and rheological properties of the polymer chains. Therefore, nanoclay addition should decrease the polymer MFI in polar polymers. The MFI values of PP/PE blends with and without different surface modifications of nanoclay are given in Fig. 2. These results reveal that penetration of polymer chains into the interlayer space of the amino-modified organoclay is greater compared to others. Consequently, the interaction between the polymer chains and the clay sheets should be stronger in it compared to others. The presence of interactions between the polymer chains and the kaolinite surface may affect the mobility and the rheological properties of the polymer chains.

The MFI values of PP/PE blends with and without fillers at different loadings of nanoclay are given in Fig. 2. These values appear to be decreasing with increase in filler loading particularly for amino-modified clay at 2 wt% of the filler. As it is shown in Fig. 2, the polymer MFI reduced significantly at filler loading of 2 wt%. This result reveals that the penetration of the polymer chains into the interlayer space of the organoclay is greater in clay nanocomposites compared to pure blends. Consequently, the interaction between the polymer chains and the kaolinite sheets should be stronger in composites and this may be the reason for decrease in MFI and enhancement in mechanical properties [44].

Thermal stability

In most cases, the incorporation of clay into the polymer matrix is found to enhance the thermal stability. The thermal stability of the nanocomposites has been investigated using TGA. Table 8 presents the results of TGA of PP/PE nanocomposites. The nanocomposites were prepared with both modified and unmodified nanokaolin clay containing 2 wt% nanoclay content. The temperature at which degradation begins (onset), the temperature at which 10 % degradation occurs, the temperature at which 50 % degradation occurs which is the midpoint of degradation process, and the temperature at which 80 % degradation occurs, which is a measure of complete degradation are recorded. It can be observed that both types of clay nanocomposites show higher degradation temperature than the pure PP/PE. Pure

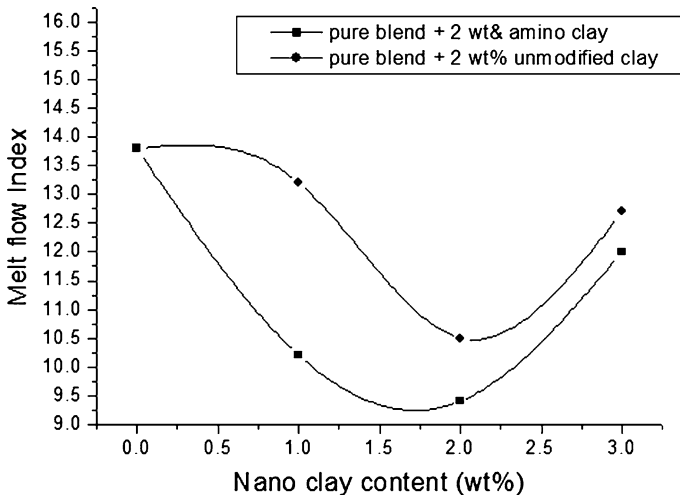


Fig. 2 Melt flow index curves of PP/PE/N100 and PP/PE/N100A at various filler loadings

Table 8 TGA results for PP/PE (80/20) clay nanocomposites

Samples	T_{onset} (°C)	10 % mass loss (°C)	50 % mass loss (°C)	80 % mass loss (°C)
Pure blend	353	400	459	482
Blend + 2 wt% unmodified clay (N100)	364	432	482	654
Blend + 2 wt% amino-modified clay (N100A)	402	444	486.66	780

blend shows an onset degradation temperature of 353 °C. For unmodified clay, this temperature shifts to 364 °C, and the corresponding value for amino-modified clay nanocomposite is 402 °C. The temperatures at which weight loss reaches 50 and 80 % drastically shift to higher temperatures upon the addition of kaolin clay.

Thermogravimetric analysis thermograms of neat PP/PE (80/20) nanocomposites with two different modified nanoclays are illustrated in Fig. 3. Improved thermal stability of nanocomposites can be attributed to the decreased permeability of oxygen caused by the partial exfoliation of the clay in the nanocomposites. This may result in the formation of highly charred carbonaceous ash cumulating on the nanocomposites surface. The charred surface layer formed during decomposition shields the thermal shock due to heat penetration to the underlying material; on the other hand, such cumulative char layer tends to retard diffusion of O_2 and volatile products through nanocomposites [21, 24, 38, 39, 43–45].

Dynamic mechanical behavior

Dynamic mechanical analyzer is used to study the relaxation in polymers. The DMA measurement consists of the observation of time-dependent deformation behavior of a sample under periodic, mostly sinusoidal deformation force with small

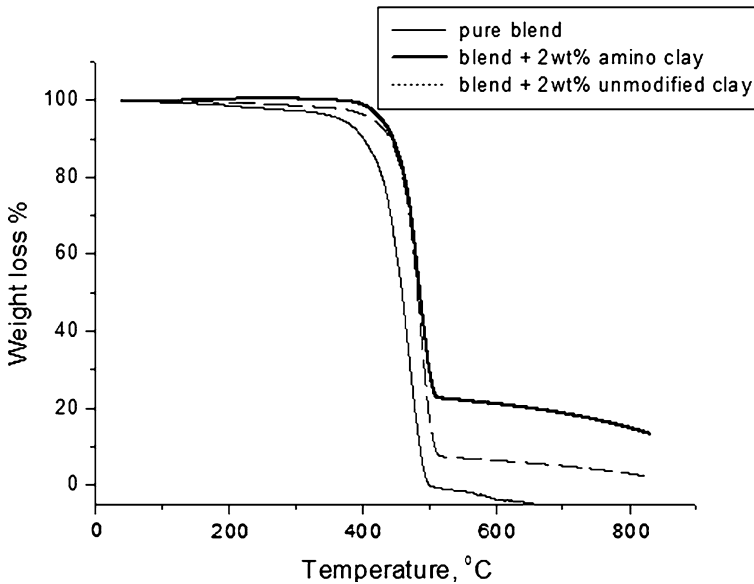


Fig. 3 TGA thermograms of neat PP/PE, PP/PE/N100, PP/PE/N100A

amplitudes. Thus, it is possible to calculate storage modulus (E') as a function of temperature and deformation frequency. The analysis of storage modulus curve is very useful in ascertaining the performance of the sample under cyclic stress and temperature. Figure 4 compares dynamic storage modulus curves of nanocomposites with two different modifications of nanokaolinite clay with PP/PE pure blend. PP/PE clay nanocomposites exhibit higher storage moduli over the entire temperature range of study (40–110 °C) than PP/PE pure blend. As can be seen from the figure, the nanocomposites with amino silane-modified clay (N100A) shows noticeably higher values of storage modulus over the range of temperature. This further shows the overall superiority of modified kaolinite clay in improving the mechanical behavior of the blend. This observation clearly illustrates the effect of surface modification of nanoclay in the intercalation of the polymer in clay sheets, leading to dispersion of clay platelets in the polymer matrix. The enhancement of storage modulus strongly depends on the aspect ratio of the dispersed clay particles and the intercalation of polymer chains inside the clay sheets [24, 38, 39, 46]. When a polymer matrix is reinforced with rigid filler particles, the polymer interface adjacent to the clay particle is highly restrained mechanically. Active surface area of the filler increases because of the intercalation of the polymer chains inside the clay galleries. Polymer chains inside the clay galleries are immobilized and the effective immobilization of these chains is responsible for the enhancement of the hydrodynamic storage modulus.

To clarify the effect of clay on E' , the storage modulus of polymer–clay nanocomposites relative to that of pure blend at different temperatures is enumerated in Table 9 (relative modulus = $E'_{\text{nanocomposites}}/E'_{\text{pure blend}}$). Apparently,

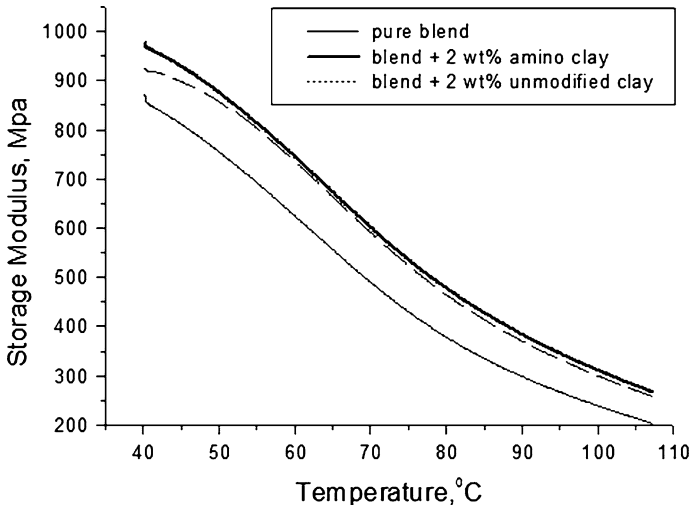


Fig. 4 Storage modulus of PP/PE, PP/PE/N100 and PP/PE/N100A

Table 9 Relative storage modulus $E'_{\text{nanocomposites}}/E'_{\text{pure blend}}$

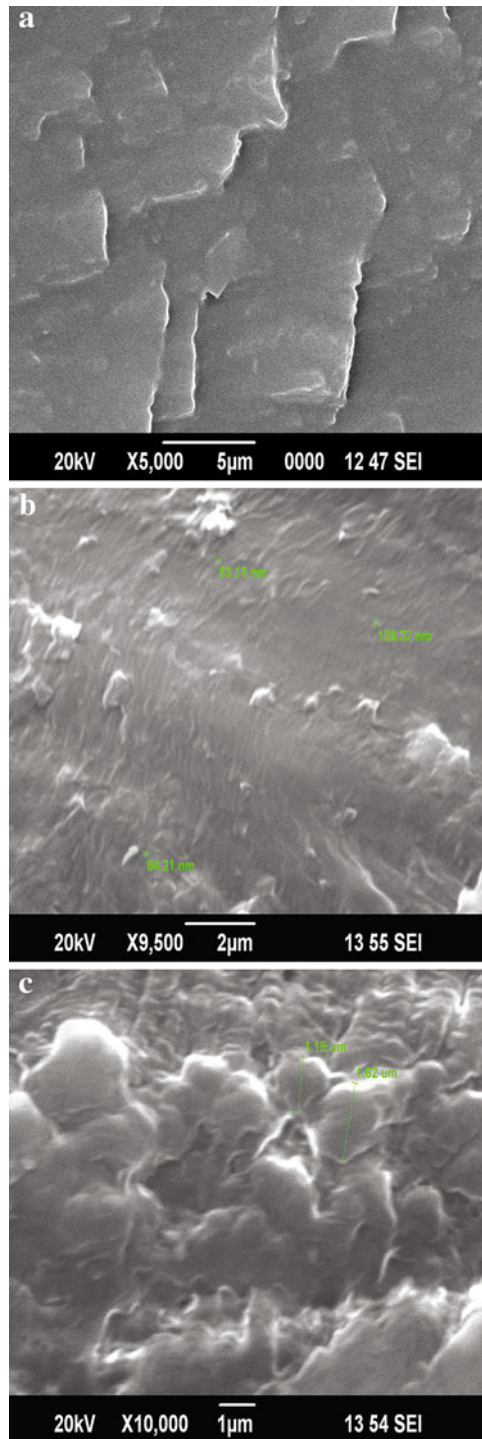
Sample	$E'_{\text{nanocomposites}}/E'_{\text{pure blend}}$			
	40 °C	60 °C	80 °C	100 °C
Pure blend + 2 wt% amino clay	1.12	1.19	1.26	1.30
Pure blend + 2 wt% unmodified clay	1.06	1.18	1.23	1.25

the relative modulus of the clay composites is higher than unity over the entire range of temperature, which is considered the real reinforcing effect of nanoclays. It is observed that the reinforcing effect of nanoclay on the storage modulus is significant at higher temperature ranges [38].

Morphological characterization

Scanning electron microscopy is an effective means for the morphological investigation of composites. Through SEM study, the distribution and compatibility between fillers and matrix can be observed. The change in mechanical properties is brought by morphological change, as documented in Fig. 5, showing SEM micrographs. SEM micrograph of pure blend (PP/PE) is shown in Fig. 5a. The fractured surface of pure blend is relatively smooth, homogenous with no separation of continuous and dispersed phases, and therefore exhibits good compatibility between the two blended phases. The tensile fractured surface of PP/PE/N100A is shown in Fig. 5b. It is possible to see smooth surface with better dispersion and homogeneity in Fig. 5b. The SEM morphology of fracture surface of PP/PE/N100 unmodified clay nanocomposites is shown in Fig. 5c. Some amount of improper mixing and reduction in compatibility is seen (Fig. 5c) for the nanocomposites

Fig. 5 **a** SEM image of PP/PE pure blend. **b** SEM image of PP/PE/N100A. **c** SEM image of PP/PE/N100



containing unmodified nanoclay (N100), compared with Fig 5b. There is no agglomeration and voids in the composites containing modified nanoclay (Fig 5b). This may be the reason for greater enhancement in mechanical properties for composites with modified nanoclay containing amino silane-modified clay edges. Similar morphological observation is reported in some earlier research papers [16, 17, 39, 48, 49].

X-ray diffraction (XRD) is extremely useful to study the structure and morphology of polymer nanocomposites. It provides information on the changes of the interlayer spacing of the clay upon the formation of nanocomposites. Clays and organoclays show a characteristic peak in XRD analysis due to their regular layered structures. The peak is indicative of the platelet separation or *d*-spacing in clay structure. Any change in the interlayer or *d*-spacing of a clay lattice by organic modification or polymer intercalation causes the change in the position, broadness and intensity of the characteristic peak in XRD spectra. According to the Bragg's law, increasing of *d*-spacing results in the broadening and shifting of related XRD peak toward lower diffraction angles 2θ . By monitoring the position 2θ , shape and intensity of the characteristic peak for organoclay in nanocomposite structure, it is possible to determine the degree of intercalation/exfoliation. Thus, the formation of an intercalated structure should result in a decrease of 2θ , indicating an increase in *d*-spacing. The interlayer *d*-spacing observed by XRD for polymer–clay nanocomposites has been used to describe the nanoscale dispersion of clay in the polymer matrix [47, 48]. From 2θ values, *d*-spacing is calculated by Bragg's equation $n\lambda = 2d \sin \theta$. Figure 6 shows XRD patterns of unmodified clay (N100), amino-modified clay (N100A), PP/PE pure blend and its nanocomposites reinforced with both unmodified and amino-modified nanokaolin clays at 2 wt%. The original basal reflection peaks for N100 and N100A are 12.41° and 12.275° , which correspond to intergallery spacing of 7.09 and 7.204 nm. Characteristic peak for PP/PE/N100 is 12.224° corresponding to a *d*-spacing of 7.234 nm and that of PP/PE/N100A nanocomposites is 11.884° and has a *d*-spacing of 7.44 nm. The increase in *d*-spacing in PP/PE/N100A indicates that some PP/PE molecular chains are intercalated between the clay galleries, forming an intercalated structure.

The extent of nanoclay intercalation in a polymer nanocomposite depends on three important factors: clay–clay interaction, polymer–surfactant interaction and polymer–clay interaction. It is reported that some surfactants can weaken clay–clay interaction to allow polymer interaction between clay sheets [39]. Incorporating surfactant with hydrophobic tails on the clay surface will efficiently reduce clay–clay interaction. During melt blending, this will facilitate the ability of PP/PE chains to intercalate in between the clay galleries.

Conclusions

The study shows that kaolinite clay, a cheap and abundantly available mineral, can be used as efficient reinforcing filler in nanodimension in the processing of PP/PE blend. The nano composite can be prepared by melt blending process. The optimum processing conditions are mixing temperature 160°C , torque 50 rpm and nanoclay

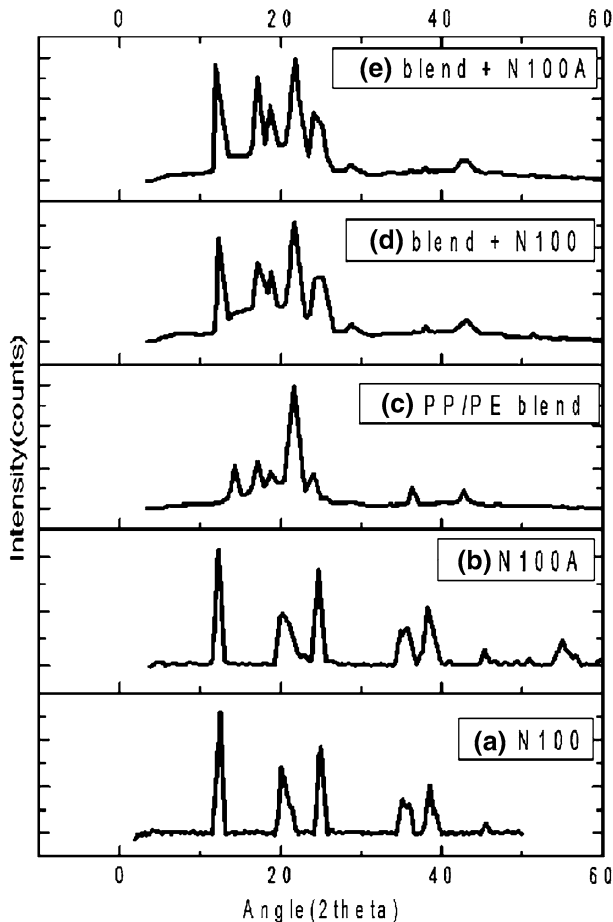


Fig. 6 XRD patterns of *a* unmodified nanoclay (N100), *b* amino-modified nanoclay (N100A), *c* PP/PE pure blend, *d* PP/PE blend/N100 nanocomposite, *e* PP/PE blend/N100A nanocomposite

loading 2 wt%. Box–Behnken method of design of experiments can be effectively utilized to optimize the variables and modeling in a single-step process [48]. Even though better mechanical properties than pure blend PP/PE are obtained for composites containing unmodified nanokaolinite clay, the mechanical and thermal properties are greatly improved on addition of modified clay with amino silane group. The composite containing modified nanoclay is found to have a greater homogenous structure. The technique provides a method for efficient utilization of nanokaolinite clay and a profitable way to produce a new engineering material from PP and PE.

Acknowledgments The authors wish to thank the organization CERD (Centre for Engineering Research and Development), Government of Kerala, India for the financial support extended to this research under the project CERD/2010/RSM (32).

References

1. Oya A, Kurokawa Y, Yasuda H (2000) Factors controlling mechanical properties of clay mineral/polypropylene nanocomposites. *J Mater Sci* 35:1045
2. Peter R, Hansjorg N, Stefen K, Rainer B, Ralf T, Rolf M (2000) Polypropylene/organoclay nanocomposite formation: influence of compatibilizer functionality and organoclay modification. *Macromol Mater Eng* 275:8
3. Pegoretti A, Dorigato A, Penati A (2007) Tensile mechanical response of polyethylene-clay nanocomposites. *Express Polym Lett* 1(3):123–131
4. Lei SG, Hoa SV, Ton That M-T (2006) Effect of clay types on the processing and properties of polypropylene nanocomposites. *Compos Sci Technol* 66:1274–1279
5. Dong Y (2008) Multiscale effects on deformation mechanisms of polymer nanocomposites: experimental characterization and numerical study. PhD Thesis, University of Auckland
6. Deenadayalan E, Vidhate S, Lele A (2006) Nanocomposites of polypropylene impact copolymer and organoclays: role of compatibilizers. *Polym Int* 55(11):1270–1276
7. Alexandre M, Dubois P (2006) Polymer-layered silicate nanocomposites: preparation, properties and uses of a new class of materials. *Mater Sci Eng* 28:1 (2000)
8. Baniyadi H, Ramazani SA, Nikkiah JS (2010) Investigation of in situ prepared polypropylene/clay nanocomposites properties and comparing to melt blending method. *Mater Des* 31:76–84
9. Gilman JW, Jackson CL, Morgan AB, Harris R (2000) Flammability properties of polymer-layered-silicate nanocomposites. *Polypropyl Polystyr Nanocomp Chem Mater* 12:1866–1873
10. Vaiziri HS, Omarai IA, Abadyan M, Mortezaei M, Yousefi N (2011) Thermophysical and rheological behaviour of polystyrene/silica nanocomposites: investigation of nanoparticle content. *Mater Des* 32:4537–4542
11. Venkatesh GS, Deb A, Ajay K, Shakti SC (2012) Effect of nanoclay content and compatibilizer on viscoelastic properties of montmorillonite/polypropylene nanocomposites. *Mater Des* 37:285–291
12. Hejazi I, Sharif F, Garmabi H (2011) Effect of material and processing parameters on mechanical properties of polypropylene/ethylene-propylene-diene-monomer/clay nanocomposites. *Mater Des* 32:3803–3809
13. Hernandez JCR, Sanchez MS, Ribelles LG, Pradas M (2007) Polymer-silica nanocomposites prepared by sol-gel technique; nanoindentation and tapping mode AFM studies. *Eur Polym J* 43:2775–2783
14. Ray SS, Okamoto M (2003) Polymer/layered silicate nanocomposites: a review from preparation to processing. *Prog Polym Sci* 28:1539–1544
15. Hui S, Chathopadhyay S, Chaki TK (2010) Thermal and thermo-oxidative degradation study of a model LDPE/EVA based TPE system: effect of nano silica and electron beam irradiation. *Polym Compos* 31(8):1387–1397
16. Akhlaghi S, Sharif A, Kalae M, Elahi A, Pirzadeh M, Mazinani S, Afshari M (2012) Effect of stabilizer on the mechanical, morphological and thermal properties of compatibilized high density polyethylene/ethylene vinyl acetate copolymer/organoclay nanocomposites. *Mater Des* 33:273–283
17. Mosleh Shirazi S, Janghorban K (2012) Investigation of physical and chemical properties of polypropylene hybrid nanocomposites. *Mater Des* 34:474–478
18. Dayama N, Bhabani KS (2012) Microstructural correlation to micromechanical properties of polyamide-6/low density polyethylene-grafted-maleic anhydride/nanoclay ternary nanocomposites. *Mater Des* 33:510–522
19. LV Z, Yang Y, Wu R, Tong Y (2012) Design and properties of a novel nucleating agent for isotactic polypropylene. *Mater Des* 37:73–78
20. Zare Y, Garmabi H, Sharif F (2011) Optimization of mechanical properties of PP/nanoclay/CaCO₃ ternary nanocomposite using response surface methodology. *J Appl Polym Sci* 122:3188–3200
21. Qiu Z-C, Zhang J-J, Huang C-L, Niu Y, Yang K-K, Wang Y-Z (2012) The influence of the surface character of the clays on the properties of poly(*p*-dioxanone)/fibrous clay nanocomposites. *J Appl Polym Sci* 125:E247–E259
22. Gunning MA, Istrate OM, Geever LM, Lyons JG, Blackie P, Chen B, Higginbotham CL (2012) The effect of maleic anhydride grafting efficiency on the flexural properties of polyethylene composites. *J Appl Polym Sci* 124:4799–4808

23. Mandal S, Alam S (2012) Studies on the mechanical, thermal and morphological properties of poly(ether ether ketone)/poly(ether sulfone)/barium titanate nanocomposites: correlation of experimental results with theoretical predictive models. *J Appl Polym Sci* 126:724–733
24. George TS, Krishnan A, Joseph N, Anjana R, George KE (2012) Effect of maleic anhydride grafting on nanokaolin clay reinforced polystyrene/high density polyethylene blends. *Polym Compos*. doi:10.1002/pc.22276
25. Vijayalakshmi NS, Murthy RAN (1992) Modification of polyethylene by unsaturated compounds. *J Appl Polym Sci* 44:1377–1382
26. Dennis HR, Hunter DL, Chang D, Kim S, White JL, Cho JW, Paul DR (2001) Effect of melt processing condition on the extend of exfoliation in organo-clay based nanocomposites. *Polymer* 42:9513–9522
27. Vaia RA, Giannelis EP (1997) Lattice of polymer melt intercalation in organically modified layered silicates. *Macromolecules* 30:7990–7999
28. Yu ZZ, Yang M, Zhang Q, Zhao C, Mai YWD (2003) Dispersion and distribution of organically modified montmorillonite in nylon-66 matrix. *J Polym Sci Polym Phys* 41:1234–1243
29. Chrissopoulou K, Anastasidis SH (2011) Polyolefin/layered silicate nanocomposites with functional compatibilizers. *Eur Polym J* 47:600–613
30. Erdem Yalc Inkaya S, Yildiz N, Sacak M, Calimli A (2010) Preparation of polystyrene/montmorillonite nanocomposites: optimization by response surface methodology. *Turk J Chem* 34:1–12
31. Ghasemi I, Karrabi M, Mohammadi M, Azizi H (2010) Evaluating the effect of processing conditions and organoclay content on the properties of styrene-butadiene rubber/organoclay nanocomposites by response surface methodology. *Express Polym Lett* 4:62–70
32. Balachandran M, Lisha PS, Mulaleekrishnan R, Bhagawan SS (2010) Modeling NBR- layered silicate nanocomposites: a DoE approach. *J Appl Polym Sci* 118:3300–3310
33. ASTM D638-94b (1995) Tensile properties of plastics. Annual book of American Society for Testing and Materials (ASTM) standards
34. ASTM D790-92 (1995) Standard test method for flexural properties of unreinforced and reinforced plastics and electrical insulating materials. Annual book of American Society for Testing and Materials (ASTM) standards
35. ASTM D 256-10 (1995) Standard test method for determining Izod pendulum impact resistance of plastics. Annual book of American Society for Testing and Materials (ASTM) standards
36. ASTM D 1238-10. Standard test method for melt flow rates of thermoplastics by extrusion plastometer, volume 08.01. ICS number code 83.080.20 (thermoplastic material)
37. Deniz B, Ismail HB (2007) Modeling and optimization I: usability of response surface methodology. *J Food Eng* 78:836
38. Nayak SK, Mohanty S, Sushanta KS (2009) Effect of clay types on the mechanical, dynamic mechanical and morphological properties of polypropylene nanocomposites. *Polym Plast Tech Eng* 48:976–988
39. Asha KK, George TS, Anjana R, Joseph N, George KE Effect of modified kaolin clays on the mechanical properties of polypropylene/polystyrene blends. *J Appl Polym Sci* doi:10.1002/app.38043
40. Liu SL, Lu XH, Liew FY, Lim SH, Yong MS Melt processing and properties of intercalated polypropylene/organoclay nanocomposites. STR/04/004/FT
41. Kallel T, Massardier-Nageotte V, Jaziri M, Gerard J-F, Elleuch B (2003) Compatibilization of PE/PS and PE/PP blends. Effect of processing conditions and formulation. *J Appl Polym Sci* 90:2475–2484
42. Homminga D, Goderis B, Hoffman S, Reynaers H, Groeninckx G (2005) Influence of shear flow on the preparation of polymer layered silicate nanocomposites. *Polymer* 46:9941–9954
43. Zhang M, Lin B, Sundararaj U (2012) Effects of processing sequence on clay dispersion, phase morphology and thermal and rheological behaviours of PA6-HDPE-clay nanocomposites. *J Appl Polym Sci* 125:E714–E724
44. Abbas-Abadi MS, Haghghi MN, Yeganeh H (2012) Effect of the melt flow index and melt flow rate on the thermal degradation kinetics of commercial polyolefins. *J Appl Polym Sci* 126:1739–1745
45. Nigam V, Soni H, Saroop M, Verma GL, Bhattacharya AS, Setua DK (2012) Thermal, morphological and X-Ray study of polymer-clay nanocomposites. *J Appl Polym Sci* 124:3236–3244
46. Komalan C, George KE, Kumar PAS, Varughese KT, Thomas S (2007) Dynamic mechanical analysis of binary and ternary polymer blends based on nyl n copolymer/EPDM rubber and EPM grafted maleic anhydride compatibilizer. *Express Polym Lett* 10:641–653

47. Banalia K, Aicha S (2012) Properties of polypropylene/polyamide nanocomposites prepared by melt processing with a PP-g-MAH compatibilizer. *Mater Des* 34:313–318
48. Anjana R, George KE, George TS, Krishnan A (2012) Optimisation of processing conditions of PP/HDPE/nanokaolinite clay composites by response surface methodology. *Int J Plast Technol* 16(2):136–149
49. Gholamian F, Ghariban-Lavasani S, Garshasbi MM, Ansari M, Bataghv F, Moraveji A, Ranjbar Z The effects of water absorption and surface treatment on mechanical properties of epoxy nanocomposite using response surface methodology. *Polym Bull*. doi: [10.1007/s00289-013-0938-8](https://doi.org/10.1007/s00289-013-0938-8)